Peer-reviewed version available at Pathogens 2019, 8, 267; doi:10.3390/pathogens8040267

Article

β-HPV 8E6 Attenuates ATM and ATR Signaling in Response to UV Damage

Jazmine A. Snow[1], Vaibhav Murthy[1], Dalton Dacus[1], Changkun Hu[1], Nicholas A. Wallace[1*]

[1] Division of Biology, Kansas State University, Manhattan, Kansas, 66502, USA

* Correspondence: nwallac@ksu.edu

Abstract: Given the high prevalence of cutaneous genus beta human papillomavirus (β-HPV) infections, it is important to understand how they are manipulating their host cells. This is particularly true for cellular responses to UV damage, since our skin is continually exposed to UV. The E6 protein from β-HPV (β-HPV E6) decreases the abundance of two essential UV-repair kinases (ATM and ATR). Since β-HPV E6 reduces their availability, the impact on downstream signaling events has been uncertain. We demonstrate that β-HPV E6 decreases ATM and ATR activation. This inhibition extended to XPA, an ATR target necessary for UV repair, lowering both its phosphorylation and accumulation. β-HPV E6 hinders POLη phosphorylation and foci formation, critical steps in translesion synthesis. ATM's phosphorylation of BRCA1 is also attenuated by β-HPV E6. However, β-HPV E6's hindrance of ATM/ATR signaling during UV-associated cell cycle arrest was incomplete. While there was less phosphorylation of immediate downstream targets (CHK1), events further down the cascade were not decreased. These observations are consistent with β-HPV infections making UV radiation more deleterious and support the proposed role of β-HPV in early stages of non-melanoma skin cancer development.

Keywords: genus beta human papillomavirus; ATM; ATR; nucleotide excision repair; translesion synthesis; cell cycle; UV

1. Introduction

The human papillomavirus (HPV) family is made up of 5 genera (alpha, beta, gamma, mu and nu papillomaviruses), each containing a large number of individual HPV types **[1,2]**. The division into these groups is based on differences in the major capsid gene's sequence **[3,4]**. Although all these genera contain members capable of causing disease, the alpha (α-HPV) and beta (β-HPV) genera have received the most research attention because of their connection and potential connection to cancer, respectively **[5–8]**. Certain members of the alpha papillomavirus genus are known to cause tumors in the anogenital tract and in the oral cavity **[9]**. These so-called high risk, or HR α-HPVs, cause tumors that are dependent on continued viral oncogene (HR α-HPV E6 and E7) expression, making it somewhat straightforward to connect their infections with tumorigenesis **[10,11]**.

β-HPVs are far more difficult to definitively tie to malignancies but are proposed to contribute to non-melanoma skin cancer (NMSC) development **[12]**. The difficulty in linking β-HPVs to NMSCs is that, unlike HR-α HPVs, they do not cause an infection that lingers in the tumor **[13,14]**. Their infections are more transient, lasting for months rather than decades like HR-α HPVs **[15]**. As a result, β-HPV infections are thought to act through a "hit and run" mechanism of oncogenesis **[16,17]**. This hypothesis holds that β-HPV infections act synergistically along with UV radiation to promote tumorigenic mutations that cause lasting changes to the cellular environment without being dependent on continued expression of β-HPV's putative oncogenes (β-HPV E6 and E7).

Peer-reviewed version available at Pathogens 2019, 8, 267; doi:10.3390/pathogens8040267

The "hit and run" hypothesis presents a challenge for epidemiologists that is further compounded by the fact that neither β-HPV infections nor NMSCs are rare. In fact, most people are sero-positive for at least one β-HPV and there are millions of NMSCs diagnosed each year **[18–20]**. The purposed link between β-HPV and NMSCs is best characterized in individuals with *Epidermodysplasia verruciformis* (EV), a genetic disease that is associated with an increased susceptibility to HPV infections, and in solid organ transplant recipients **[21–23]**. While a potential role in cancer warrants further investigation, the ubiquitous presence of β-HPV in our skin alone makes it important to further understand β-HPV biology.

Of β-HPV's genes, β-HPV E6 is the most well characterized **[24]**. It alters multiple cell signaling pathways including MAML1, TGFβ, NOTCH and EGFR signaling **[25–27]**. It also binds and destabilizes the cellular histone acetyltransferase, p300 **[28]**. We have previously shown p300's role as a transcription factor is required for robust expression of at least four essential DNA repair genes, including two essential repair kinases (ATM and ATR) **[29–31]**. Because of their position atop multiple repair pathways, we hypothesize that diminished ATM and ATR availability has a far-reaching impact on the ability of cells to protect themselves from UV radiation **[32–35]**.

Here, we show that β-HPV E6 decreases the phosphorylation of ATM and ATR targets, including essential members of the nucleotide excision repair (NER) and translesion synthesis (TLS) pathways. Because NER is responsible for physically removing UV-induced DNA lesions, our results offer mechanistic insight into the prior observation that β-HPV E6 delays repair of UV photo-products **[29,36]**. Specifically, β-HPV E6 reduces the ATR-dependent phosphorylation required for XPA stabilization and NER function **[37,38]**. β-HPV E6 also attenuates stabilization of POLη, the TLS polymerase most relevant for bypassing UV lesions **[39,40]**. Further, while β-HPV E6 decreases CHK1 phosphorylation and total CHK1 abundance, signaling events further downstream were not attenuated **[41]**. β-HPV E6 increases the percentage of cells in S phase with and without UV. Finally, β-HPV E6 decreases ATM activation and its ability to phosphorylate downstream targets involved in repair of double stranded DNA breaks via homologous recombination. Together these data better elucidate β-HPV E6's manipulation of UV damage repair.

2. Results

2.1. ATR, ATM and p53 Have Distinct Transcription Effector Profiles.

We have previously reported that β-HPV 8E6 decreases ATM and ATR abundance **[29,30]**. However, the extent that β-HPV 8E6 disrupts ATM and ATR signaling remains unknown. These data motivated us to characterize the extent that β-HPV 8E6 alters ATM and ATR signaling pathways. As a first step, we performed an *in silicio* screen of previously collected transcriptomic data **[42–44]**. Cell lines with ATM/ATR expression with z-scores below -2 were considered to have low expression and compared to the remaining cell lines. We focused our analysis on genes that belonged to two pathways involved in UV repair responses, namely nucleotide excision repair (NER) and translesion synthesis (TLS) as well as a few canonical ATR/ATM targets (BRCA1, CHEK1, CDC25A, and TP53) *[45–49]*. We were unable to use this analysis for CHEK2, one of the most characterized ATM targets, as there was no data available in the transcriptomic data for it. Gene expression was plotted against statistical significance in volcano plots to highlight significant robust changes in expression **(Figure 1)**.

As expected, ATM and ATR positively regulated UV responsive and canonical target genes. We complimented this approach by performing the reciprocal analysis of cells that over expressed these kinases. Like when ATM and ATR expression was low, excess ATM and ATR had a positive correlation with their established target and UV-responsive genes. **(Supplemental Figure 1)**. For

Preprints (www.preprints.org) | NOT PEER-REVIEWED | Posted: 30 September 2019 doi:10.20944/preprints201909.0338.v1

Peer-reviewed version available at Pathogens 2019, 8, 267; doi:10.3390/pathogens8040267

both over- and under-expression of ATM/ATR, the changes in all three gene expression groups were more dependent on ATM expression than ATR expression **(Figure 1, Supplemental Figure 1)**.

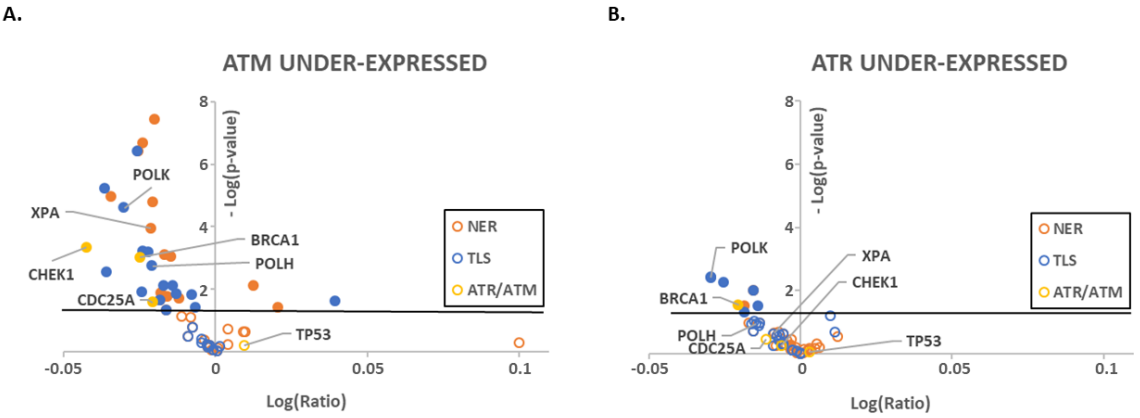

Figure 1. Under-expression of ATR/ATM mRNA leads to a decrease in UV damage repair pathways gene expression. (a) NER (orange), TLS (blue), and canonical ATR/ATM targets (yellow) mRNA expression when ATR is under expressed. Z-score less than or equal to -2. Outlined circles represent non-significant expression changes. Filled in circles represent significant expression changes. Black line represents significance cutoff (p-value less than 0.05). The right side of the graph represents increased expression and the left side of the graph represents decreased expression. X axis depicts the log of the ratio of changed versus control expression. Y axis depicts the negative log of the p-value of the changed expression. Data sets were obtained from cBioPortal. (b) NER (orange), TLS (blue), and canonical ATR/ATM targets (yellow) mRNA expression when ATM is under expressed. Z-score less than or equal to -2. Outlined circles represent non-significant expression changes. Filled in circles represent significant expression changes. Black line represents significance cutoff (p-value less than 0.05). The right side of the graph represents increased expression and the left side of the graph represents decreased expression. X axis depicts the log of the ratio of changed versus control expression. Y axis depicts the negative log of the p-value of the changed expression Data sets were obtained from cBioPortal.

Both capstone DNA repair kinases have multiple targets that they regulate primarily via phosphorylation **[33]**. p53 is preeminent among those targets for both ATM and ATR *[50]*. We have also previously shown that β-HPV 8E6 delays p53 stabilization in response to UV damage *[51]*. To understand how much of the expression profile was the result of ATM/ATR signaling through p53, we characterized expression of ATM/ATR responsive genes in cells with less p53 expression **(Table 1)**. This was distinct from both ATM and ATR expression profiles but shared some notable overlap. POLK had a positive correlation in all three settings suggesting that POLK may be regulated by ATM, ATR and p53. This includes the possibility that each regulates POLK expression independently as well as the possibility that ATM and ATR regulate POLK by stabilizing p53.

	p53	ATR	ATM
BRCA1	n.s.	++	+++
CDC25A	n.s.	n.s.	++
CHEK1	-	n.s.	+++
POLH	+++	n.s.	++
POLK	+	++	+++
XPA	-	n.s.	+++

Table 1. Repression of DNA repair signaling by down regulated ATM/ATR does not likely occur exclusively through p53. n.s. denotes a non-significant relationship. -/+ denote significant relationships p<0.05 with low magnitude. --/++ denote relationships with 0.05<p>0.001 and 0.02>log ration>0.01. ---/+++ denote relationships with p<0.001 and log ratio>0.02. (sign denotes negative and positive regulation).

2.2. β-HPV E6 Decreases ATM and ATR Activation.

These data motivated us to interrogate β-HPV E6's ability to decrease ATR/ATM signaling with in vitro systems, beginning with the ATM activation that occurs via autophosphorylation at Ser1981

(pATM). β-HPV infection occurs in keratinocytes, making them the preferred cell culture model. We used p300 abundance as a surrogate marker for β-HPV E6 expression to confirm expression of β-HPV E6 in primary keratinocytes (LXSN and β-HPV 8E6 HFKs). Since these cells are derived from patients, it was important to control for donor variability using lines derived from separate sources. To this end, we used cells that expressed β-HPV E6 in HFKs derived from a different donor's foreskin and immortalized by exogenous hTERT expression (hTERT HFKs). Probing for the HA-tag on the β-HPV 8E6 expressed in hTERT HFKs provided proof of expression **(Supplemental Figure 2)**. Finally, hTERT HFKs mimic the telomerase activation that is a common in NMSCs providing insight into β-HPV E6 phenotypes in a relevant cellular environment *[52]*.

β-HPV 8E6 decreased total and activated ATM in each of these cell lines **(Figure 2A-C)**. These differences remained over 8 hours after UV-induced ATM activation **(Figure 2B-C)**. To determine if β-HPV 8E6 prevents ATM from phosphorylating its downstream targets , we probed for two canonical ATM targets associated with the DNA damage response, Ser1423 of BRCA1 (pBRCA1) and Thr68 of CHK2 (pCHK2) *[53,54]*. β-HPV 8E6 caused aberrations in both proteins' reaction to UV **(Figure 2B-C)**. pCHK2 accumulation and total CHK2 abundance were both decreased by β-HPV 8E6. pBRCA1 levels peaked higher, but this buildup was delayed, occurring several hours after vector control levels peaked demonstrating a delayed response similar to what we have reported for p53 **[29] (Figure 2B)**. β-HPV 8E6 also decreased p53 stabilization, but we cannot distinguish whether this is an ATM or ATR effect as both kinases stabilize p53 **(Supplemental Figure 3)**. To determine if β-HPV 8E6 changed ATM's cellular position, we performed subcellular fractionation on cells before and after UV treatment. There were no robust differences in localization, suggesting that β-HPV 8E6 primarily impairs ATM activation via decreased expression and autophosphorylation **(Figure 2D)**.

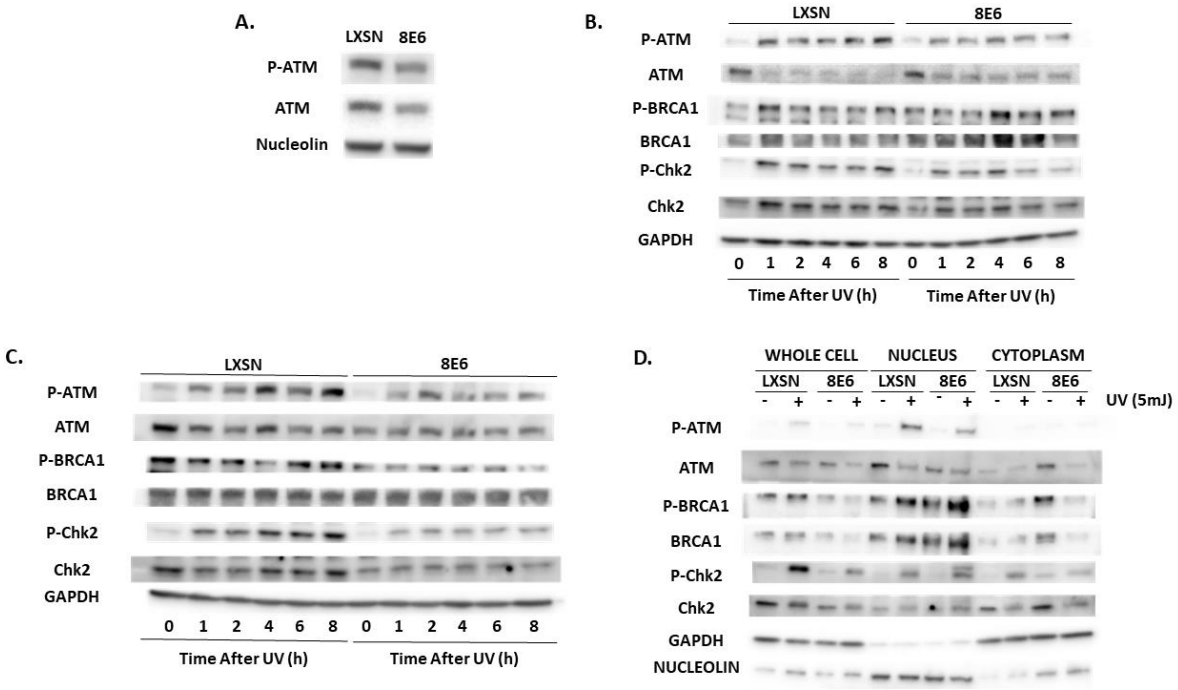

Figure 2. β-HPV 8E6 attenuates ATM activation. (a) Representative immunoblots of untreated hTERT HFKs with vector control (LXSN) and β-HPV 8E6 cell lines. Nucleolin was used as a loading control. (b) Representative immunoblots of hTERT HFKs with vector control (LXSN) and β-HPV 8E6 harvested 1-8 hours post 5mJ/cm^2 UVR. GAPDH was used as a loading control. (c) Representative immunoblots of primary HFKs with vector control (LXSN) and β-HPV 8E6 harvested 1-8 hours post 5mJ/cm^2 UVR. GAPDH was used as a loading control. (d) Subcellular fractionation of hTERT HFKs with vector control (LXSN) and β-HPV 8E6 cell line lysates harvested 6 hours post exposure to 5mJ/cm^2 UVR were observed via immunoblot. GAPDH was used as a cytoplasmic loading control and Nucleolin was used as a nuclear loading control.

Peer-reviewed version available at Pathogens 2019, 8, 267; doi:10.3390/pathogens8040267

We then moved to ATR's activation by autophosphorylation at Thr1989 (pATR). This typically occurs in response to single stranded DNA associated with replication stress *[55]*. β-HPV E6 decreased pATR in hTERT HFKs **(Figure 3A)**. pATR levels increased in vector control (LXSN) HFKs over 6 hours following UV but did not change in the presence of β-HPV E6. This resulted in notably less pATR in cells with β-HPV 8E6 after UV **(Figure 3B-C)**. Subcellular fractionation did not provide evidence that β-HPV E6 attenuated localization of pATR to the nucleus **(Figure 3D)**.

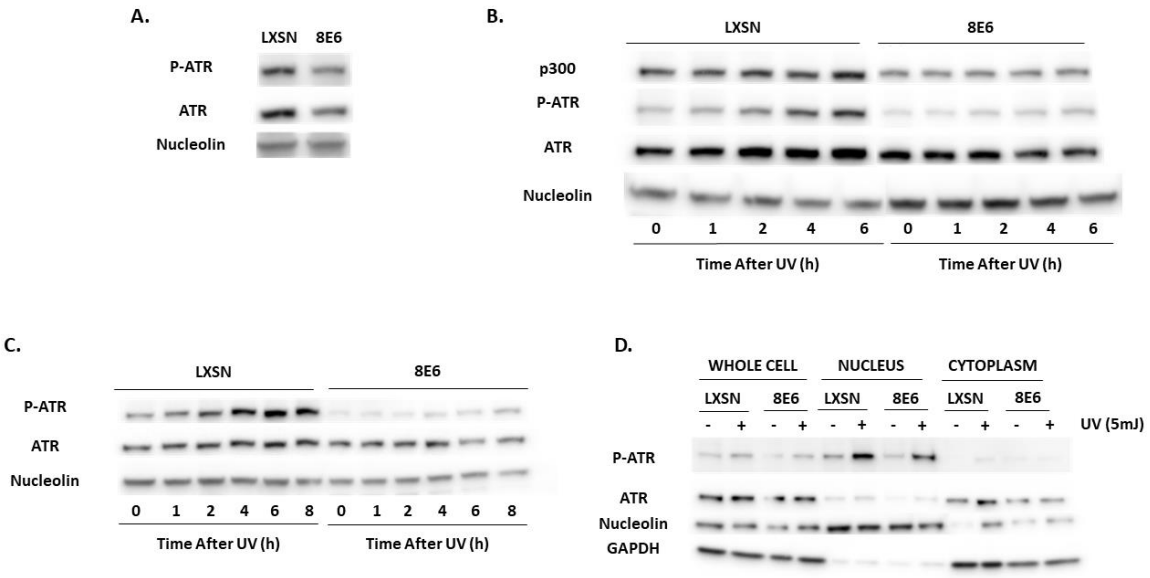

Figure 3. β-HPV 8E6 attenuates ATR activation. (a) Representative immunoblots of untreated hTERT HFKs with vector control (LXSN) and β-HPV 8E6 cell lines. Nucleolin was used as a loading control. (b) Representative immunoblots of hTERT HFKs with vector control (LXSN) and β-HPV 8E6 harvested 1-6 hours post 5mJ/cm^2 UVR. Nucleolin was used as a loading control. (c) Representative immunoblots of primary HFKs with vector control (LXSN) and β-HPV 8E6 harvested 1-8 hours post 5mJ/cm^2 UVR. Nucleolin was used as a loading control. (d) Subcellular fractionation of hTERT HFKs with vector control (LXSN) and β-HPV 8E6 cell line lysates harvested 6 hours post exposure to 5mJ/cm^2 UVR were observed via immunoblot. GAPDH was used as a cytoplasmic loading control and Nucleolin was used as a nuclear loading control.

2.3. β-HPV 8E6 decreases phosphorylation of ATR target proteins.

We continued our characterization of β-HPV 8E6's impact on UV signaling by examining ATR's most established target, CHK1 *[56]*. ATR phosphorylates CHK1 at Ser345 (pCHK1) in response to replication stress and UV *[57]*. We saw a mild increase in a replication stress marker (RPA32 at Ser8 (pRPA32)) accompanying β-HPV 8E6 expression **(Supplemental Figure 4)**. In contrast, pCHK1 was decreased by β-HPV 8E6 **(Figure 4A)**. The decrease in pCHK1 was accompanied by a reduction in total CHK1. This result is similar to a recent report **[41]**. To determine if changes in transcription might cause the decreased CHK1 abundance, RT-PCR was used to define CHEK1 transcription. β-HPV 8E6 caused a modest but non-significant decrease in CHEK1 mRNA consistent with our *in silico* data **(Figures 1 and 4B)**. Next, we probed pCHK1 and total CHK1 by immunoblot over a 6-hour time course after UV. While UV elicited a sizable increase in pCHK1 within an hour of exposure in vector control cells, β-HPV 8E6 prevent all but a mild induction of pCHK1 **(Figure 4C-D)**. These changes were independent of foreskin donor or hTERT activation.

CHK1 coordinates cell cycle progression at the G1-S boundary **[58]**. To determine if β-HPV 8E6 diminished phosphorylation downstream of CHK1 activation, we defined the phosphorylation status of CHK1 targets, beginning with CDC25A **[59]**. This dual–specificity protein phosphatase removes inhibitory phosphorylates from cyclin-dependent kinases like CDK2 and other regulatory factors like CDC2, allowing them to promote cell cycle progression. Highlighting the key role of

CDC25A in tumorigenesis, it is frequently overexpressed in cancer cells and associated with poor cancer patient outcomes **[60]**. In response to UV, pCHK1 phosphorylates CDC25A increasing its proteasome-mediated turnover **[59]**. To our surprise, β-HPV 8E6 increased total CDC25A abundance as well as the protein's phosphorylation at Thr507 (pCDC25A) **(Figure 4E)**. After UV, pCDC25A abundance increased in control cells. β-HPV 8E6 limited the accumulation of pCDC25A. Further, total CDC25A levels remained higher in the presence of β-HPV 8E6 **(Figure 4E)**. Interestingly, pCDC2 (at Thr14) levels rose higher in β-HPV 8E6 expressing cells than control cells **(Figure 4E)**. This could be explained either by β-HPV 8E6 not completely inhibiting ATR signaling or by redundant kinase activity. β-HPV 8E6 subtly changed cell cycle distribution, increasing the percentage of cells in S phase **(Figure 4F)**.

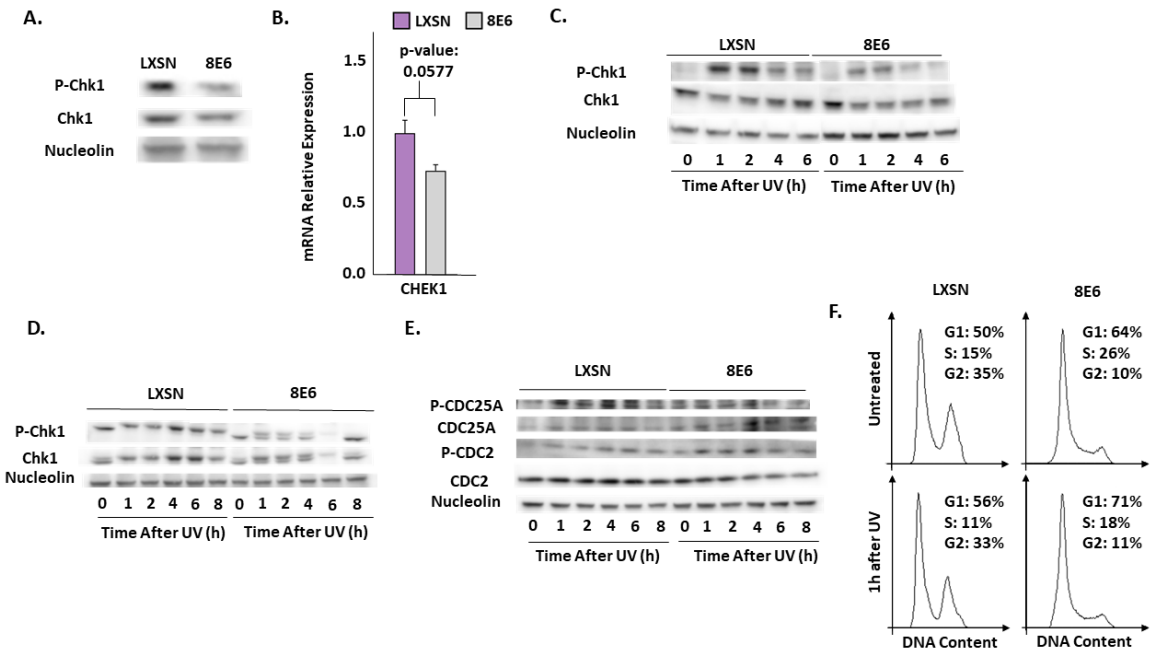

Figure 4. β-HPV 8E6 attenuates Chk1 phosphorylation. (a) Representative immunoblots of untreated hTERT HFKs with vector control (LXSN) and β-HPV 8E6 cell lines. Nucleolin was used as a loading control. (b) mRNA expression level of CHEK1 in vector control (LXSN) and β-HPV 8E6 expressing primary HFKs as measured by RT-qPCR and normalized towards the expression level of β-actin. Data shown in figures are the means of ±SE of three independent experiments. (c) Representative immunoblots of hTERT HFKs with vector control (LXSN) and β-HPV 8E6 harvested 1-6 hours post 5mJ/cm² UVR. Nucleolin was used as a loading control. (d) Primary HFK Chk1 UV timecourse (e) Representative immunoblots of hTERT HFKs with vector control (LXSN) and β-HPV 8E6 harvested 1-8 hours post 5mJ/cm² UVR. Nucleolin was used as a loading control. (f) Cell cycle analysis of hTERT HFKs with LXSN vector control and β-HPV 8E6 1h post 5mJ/cm² UVR.

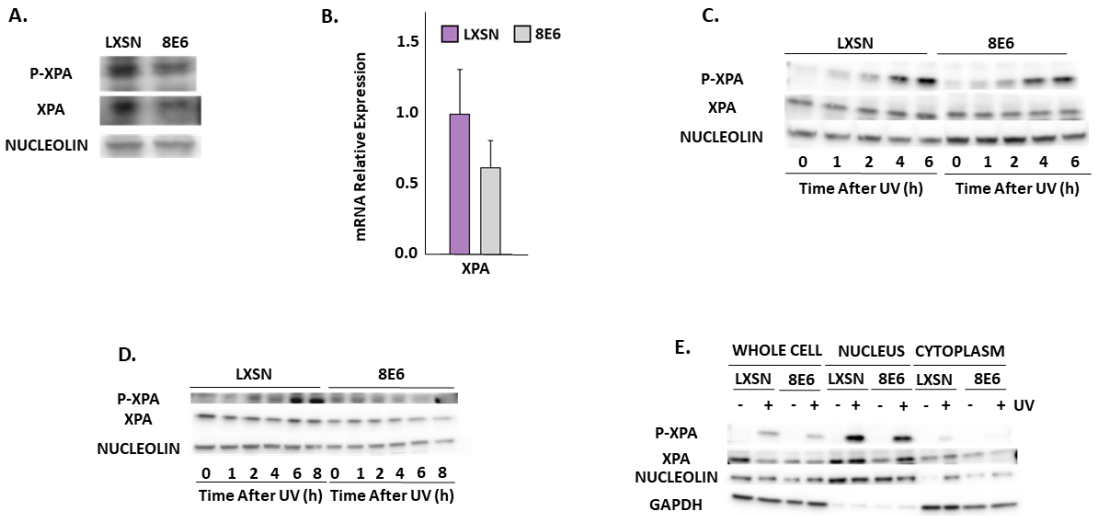

Peer-reviewed version available at Pathogens 2019, 8, 267; doi:10.3390/pathogens8040267

Figure 5. β-HPV 8E6 attenuates XPA phosphorylation. (a) Representative immunoblots of untreated hTERT HFKs with vector control (LXSN) and β-HPV 8E6 cell lines. Nucleolin was used as a loading control. (b) mRNA expression level of XPA in vector control (LXSN) and β-HPV 8E6 expressing primary HFKs as measured by RT-qPCR and normalized towards the expression level of β-actin. Data shown in figures are the means of ±SE of three independent experiments. (c) Representative immunoblots of hTERT HFKs with vector control (LXSN) and β-HPV 8E6 harvested 1-6 hours post 5mJ/cm² UVR. Nucleolin was used as a loading control. (d) Representative immunoblots of primary HFKs with vector control (LXSN) and β-HPV 8E6 harvested 1-8 hours post 5mJ/cm² UVR. Nucleolin was used as a loading control. (e) Subcellular fractionation of hTERT HFKs with vector control (LXSN) and β-HPV 8E6 cell line lysates harvested 6 hours post exposure to 5mJ/cm² UVR were observed via immunoblot. GAPDH was used as a cytoplasmic loading control and Nucleolin was used as a nuclear loading control.

ATR promotes NER by phosphorylating and stabilizing XPA in response to UV [61,62]. We measured total XPA and XPA phosphorylation at Ser196 (pXPA) by immunoblot. β-HPV 8E6 lowered both total XPA and pXPA **(Figure 5A)**. A small but insignificant decrease in XPA mRNA accompanied β-HPV 8E6 expression indicating that this decrease in abundance is not likely due to reduced transcription **(Figure 5B)**. Unlike previous phenotypes, β-HPV 8E6's ability to attenuate phosphorylation of XPA after UV seems limited by hTERT activation **(Figure 5C-D)**. To make sure that our primary keratinocyte result was not an anomaly, we observed XPA phosphorylation in a previously described osteosarcoma cell line expressing β-HPV 8E6. β-HPV 8E6 attenuated XPA phosphorylation in these cells **(Supplemental Figure 5)**. Consistent with our previous experiments, we found that β-HPV 8E6 did not affect XPA's distribution in subcellular fraction experiments. **(Figure 5E)**. However, immunofluorescence microscopy also showed β-HPV 8E6's ability to reduce nuclear localization of XPA after UV **(Supplemental Figure 6).**

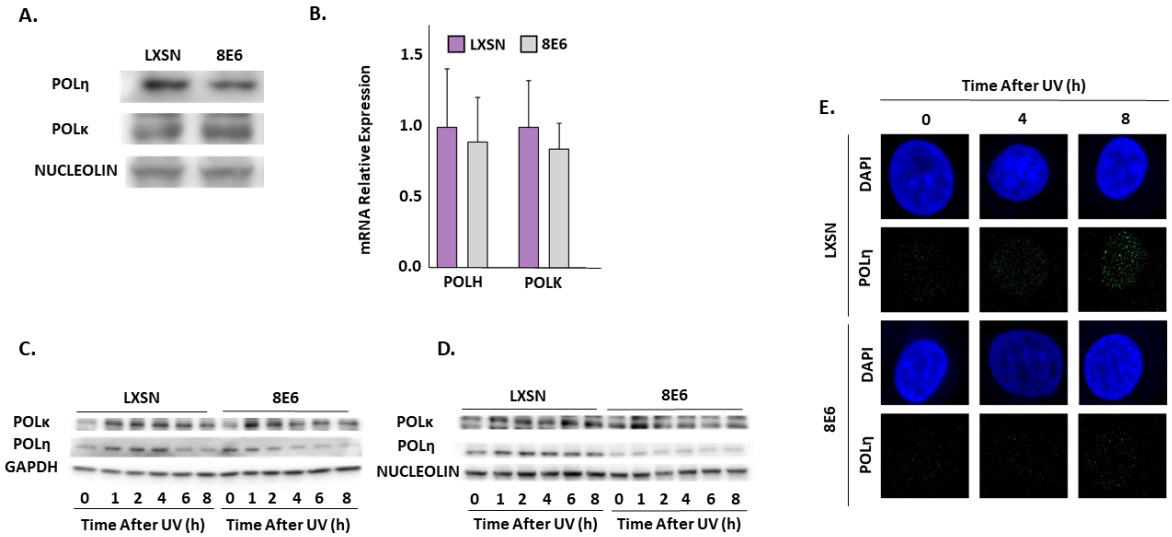

Figure 6. β-HPV 8E6 attenuates POLη abundance. (a) Representative immunoblots of untreated hTERT HFKs vector control (LXSN) and β-HPV 8E6 cell lines. Nucleolin was used as a loading control. (b) mRNA expression level of POLH and POLK in vector control (LXSN) and β-HPV 8E6 expressing primary HFKs as measured by RT-qPCR and normalized towards the expression level of β-actin. Data shown in figures are the means of ±SE of three independent experiments. (c) Representative immunoblots of hTERT HFKs with vector control (LXSN) and β-HPV 8E6 harvested 1-8 hours post 5mJ/cm² UVR. GAPDH was used as a loading control. (d) Representative immunoblots of primary HFKs with vector control (LXSN) and β-HPV 8E6 harvested 1-8 hours post 5mJ/cm² UVR. Nucleolin was used as a loading control. (e) Representative immunofluorescence microscopy images of hTERT HFKs. POLη (green) and nuclei stained (blue) with DAPI.

Peer-reviewed version available at Pathogens 2019, 8, 267; doi:10.3390/pathogens8040267

Figure 1 suggests that β-HPV E6 reduces POLη expression **[40,63]**. This is supported by our immunoblot analysis that shows β-HPV 8E6 causes a sizable decrease in POLη **(Figure 6A)**. In contrast, we found that POLκ abundance, another TLS polymerase, was not significantly altered by β-HPV 8E6 **(Figure 6A) [64]**. β-HPV 8E6 caused an insignificant decrease in POLH (gene for POLη) expression **(Figure 6B)**. Previous reports have shown that POLη stability is dependent on ATR phosphorylation during UV damage **[39]**, therefore we hypothesized that POLη would be less stable in β-HPV 8E6 expressing cells. β-HPV 8E6 does not change the abundance of other TLS proteins, such as RAD18 and ubiquinated PCNA **(Supplemental Figure 7)**. Exposure to UV increased the abundance of POLη and POLκ in control cells **(Figure 6C-D)**. While β-HPV 8E6 prevented POLη induction, POLκ rose more sharply after UV **(Figure 6C-D)**. This may represent a compensatory response. Neither of these phenotypes were altered by hTERT activation and both were consistent among cells derived from different donors **(Figure 6C-D)**. There are likely functional ramifications of the reduced POLη abundance as immunofluorescence microscopy demonstrated that β-HPV 8E6 reduced UV-induced POLη nuclear foci **(Figure 6E).**

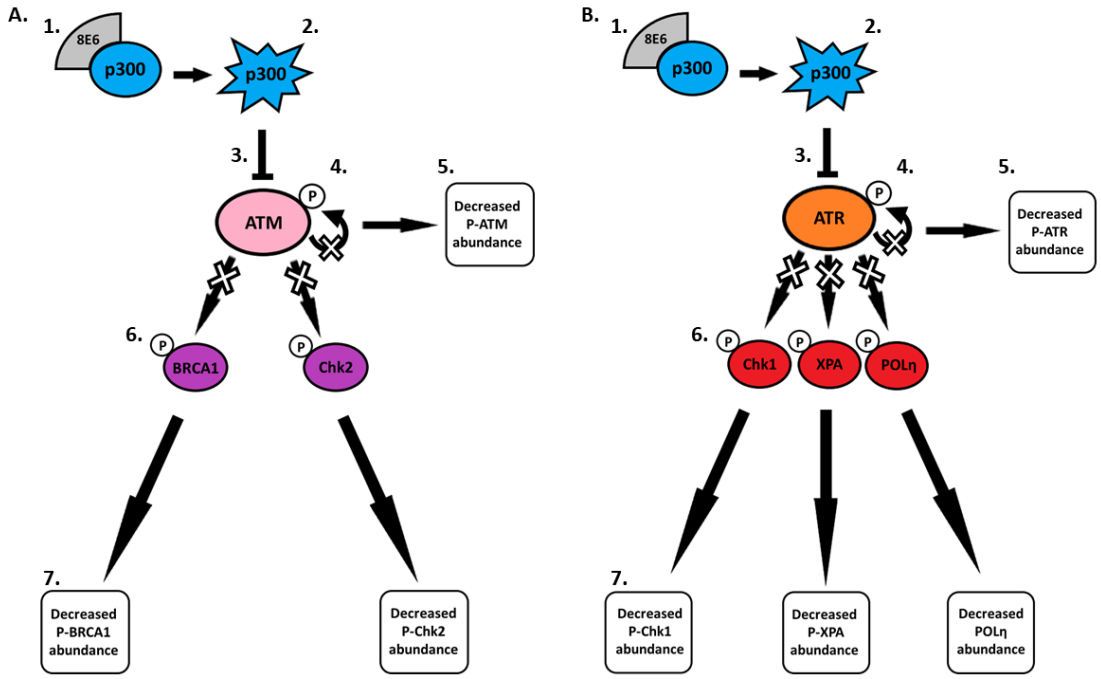

Figure 7. Schematic diagram of the effects of β-HPV 8E6 on downstream ATM and ATR targets. (a) β-HPV 8E6 binds to p300 (1) causing p300 to become destabilized and subsequentially degraded (2). The decrease in p300 levels leads to less ATM transcription (3). This leads to a decrease in ATM autophosphorylation (4) resulting in less activated ATM available (5). Limited availability of activated ATM leads to a decrease in ATM-dependent phosphorylation of downstream proteins (6) causing changes in β-HPV 8E6 infected cells (7). (b) β-HPV 8E6 binds to p300 (1) causing p300 to become destabilized and subsequentially degraded (2). The decrease in p300 levels leads to less ATR transcription (3). This leads to a decrease in ATR autophosphorylation (4) resulting in less activated ATR available (5). Limited availability of activated ATR leads to a decrease in ATR-dependent phosphorylation of downstream proteins (6) causing changes in β-HPV 8E6 infected cells (7).

3. Discussion

Pre-clinical studies and observations in immunocompromised people with NMSC support the role of β-HPV in NMSC development **[65,66]** . Yet, gaps in the molecular details of how β-HPV E6 changes the cellular environment remain. To address this challenge, we defined how β-HPV 8E6's reduction of ATR and ATM impacted cell signaling in response to UV. This work expands the breadth of known UV-responsive pathways impaired by β-HPV E6 to include nucleotide excision

repair and translesion synthesis **(Figures 5 and 6, respectively)**. We also provide details of how β-HPV 8E6 causes aberrant cell cycle regulation and the limitations of its impairment of ATR signaling. Despite substantial decreases in Chk1 phosphorylation, the S phase population was only mildly increased. This subtly may be explained by β-HPV 8E6's inability to attenuate further downstream signaling events (such as CDC2 dephosphorylation) **(Figure 4)**. Figure 7 details the β-HPV E6 induced changes to DNA repair and cell cycle regulation described throughout this paper.

The implications of these data are broad. CRISPR/CAS9 and similar genome editing technologies have opened doors to learning about cellular biology **[67]**. In some cases, this approach is superior to using viral oncogenes as it has a potential to reduce off-target effects. However, our data demonstrate that viral oncogenes can offer a subtler manipulation of cell signaling illustrating situations where viral oncogenes remain useful tools for learning about cellular biology. Expressing β-HPV 8E6 in skin cells demonstrated that attenuated, but not vacated, ATM and ATR expression leave cells capable of inducing at least one TLS polymerase (POLκ). While this likely facilitates lesion bypass and prevents some replication fork collapse, TLS is an inherently mutagenic pathway **[68]**. TLS polymerases bypass DNA lesions by adding untemplated base pairs to the growing strand. Instead of being by random chance, TLS polymerases have some DNA damage specificity. For example, POLη is the primary UV-responsive TLS polymerase because it is most likely to insert the correct base pairs for a UV lesion than other TLS polymerases **[69]**. As a result, substituting POLκ for POLη comes at an increased the risk of mutation **[70]**. With DNA repair inhibitors on the horizon for cancer therapeutics, this type of information is essential to fully appreciate the consequences of transient repair inhibition.

Studying β-HPV E6 also provided insight into telomerase biology. hTERT immortalization is a fantastic tool that makes difficult cell lines far more trackable by extending their lifespan **[71]**. There are also times that studying cells that overexpress hTERT is biologically relevant. For example, telomerase activation is an essential step in many cancers, including NMSCs **[52,72–75]**. We mimic this phenotype using hTERT HFKs **[75]**. Our data suggest that researchers should be careful with this tool, because overexpression of telomerase can also mask phenotypes. We do not mean to detract from hTERT immortalized cell lines. Instead, we suggest being aware that telomerase activation can alter signaling provides the opportunity for further insight. For instance, our observation that β-HPV 8E6 loses its ability to hinder NER in the presence of extra telomerase activity is consistent with observations that β-HPV expression declines as premalignant skin lesion progress to NMSCs. If β-HPV's transformative phenotypes are lost as NMSCs develop and acquire telomerase activating mutations, then there would no longer be a selective pressure for the tumor to maintain viral gene expression.

Finally, we show that β-HPV 8E6 is not able to universally hinder ATR signaling. Signaling events farther downstream (CDC25A phosphorylation for example) are less effected. As we understand more about the consequences of p300 destabilization by some β-HPV E6s, we will likely encounter other examples where some ATR signaling is enough to accomplish the cell's needs. We suspect this principle will apply when β-HPV E6 reduces other key signaling proteins and may be applicable to other viral-host interactions. As a result, the continued interrogation of abrogated signaling is both warranted and necessary.

4. Materials and Methods

4.1 Antibodies:

The following primary antibodies were used: P-ATM (Ser1981)(D25E5)(Cell Signaling 13050S), ATM (11G12) (Cell Signaling 92356S), P-ATR (Thr1989) (Cell Signaling 58014S), ATR (Cell Signaling 2790S), P-BRCA1 (Ser1423)(Abcam ab90528), BRCA1 (Cell Signaling 9010S), P-CHK2 (Thr68)(C13C1)(Cell Signaling 2197S), CHK2 (Cell Signaling 2662S), P-CHK1 (Ser345)(133D3)(Cell Signaling 2348S), CHK1 (2G1D5)(Cell Signaling 2360S), P-CDC25A (Thr507)(Thermo Fisher PA512564), CDC25A (DCS121)(Thermo Fisher MA112293), P-CDC2 (Thr14)(Cell Signaling 2543S), CDC2 (Cell Signaling

77055S), P-CDK2 (Tyr15)(Fisher Scientific PA5-77907), CDK2 (78B2)(Cell Signaling 2546S), P-XPA (Ser196)(Thermo Fisher PA5-64730), XPA (5F12)(Abcam ab65963), RAD18 (Abcam ab57447), UB. PCNA (Lys164)(D5C7P)(Cell Signaling 13439S), PCNA (PC10)(Cell Signaling 2586S), POLκ (Abcam ab57070), POLη (B-7)(Santa Cruz sc-17770), P-RPA32/RPA2 (Ser8)(Cell Signaling 83745S), RPA32/RPA2 (Cell Signaling 52448S), RPA70/RPA1 (Cell Signaling 2267S), TOPBP1 (B-7)(Santa Cruz sc-271043), GAPDH (0411)(Santa Cruz sc-47724), NUCLEOLIN (C23)(MS-3)(Santa Cruz sc-8031).
The following secondary antibodies were used: Peroxidase AffiniPure Goat Anti Mouse IgG (H+L) (Jackson ImmunoResearch 115-035-003), Anti Rabbit IgG, HRP-linked (Cell Signaling 7074S), Goat anti-Rabbit IgG (H+L) Cross-Adsorbed Secondary Antibody, Goat anti-Mouse IgG (H+L) Cross-Adsorbed Secondary Antibody, Alexa Fluor 488 (Thermo Fisher A-11001), Alexa Fluor 594 (Thermo Fisher A-11012).

4.2 Cell Culture:

Primary human foreskin keratinocytes (HFKs) were isolated from neonatal human foreskins. HFKs were grown in EpiLife medium (Gibco) supplemented with calcium chloride (Gibco), human keratinocyte growth supplement (Gibco), and penicillin-streptomycin (Calsson). hTERT human foreskin keratinocytes (hTERT HFKs), provided by Michael Underbrink, are immortalized keratinocytes that constituently express telomerase (hTERT). hTERT HFKs were grown in EpiLife medium (Gibco) supplemented with calcium chloride (Gibco), human keratinocyte growth supplement (Gibco), and penicillin-streptomycin (Calsson). Multiple passages were used throughout these experiments for both cell lines. hTERT HFKs and primary HFKs both expressed the control vector (LXSN) and β-HPV 8E6; hTERT HFKs expressed HA-tagged β-HPV 8E6.

4.3 Cell Cycle Analysis:

Cells were harvested by trypsinization from 10-cm dishes, with cells being 70–90% confluent. After washing with cold 1x phosphate-buffered saline (PBS), cells were fixed with 4% paraformaldehyde (PFA) in 1xPBS for 15 min, and permeabilized in PBS containing 0.2% Triton X-100 for 30 min at room temperature. After washing with PBS, cells were resuspended in 0.2 ml of PBS and 3 μM of DAPI was added, then incubated at room temperature for 30 min in the dark [76].
Samples were analyzed by using an LSR Fortessa X20 Flow Cytometer. Cells were gated on the Forward versus Side Scatter plot to eliminate debris, and then single cells were gated by using a dot-plot showing the pulse width versus pulse area of the DAPI channel. Post-acquisition analysis was performed with Flowing software 2.5.1. [76].

4.4 Comparative Transcriptomic Analysis:

Web-based software on cBioPortal for Cancer Genomics (ww.cbioportal.org) was used to analyze RNAseq data from the Cancer Cell Line Encyclopedia [42–44].

4.5 Immunoblot:

Whole cell lysates were prepared by washing cells in cold 1XPBS before incubating on ice in complete RIPA lysis buffer (RIPA lysis buffer, protease inhibitor, phosphatase inhibitor). Then they were mechanically harvested after being exposed to 5mJ/cm^2 for the appropriate time if necessary. Lysates were then centrifuged for higher purification and protein concentration was determined via BCA assay. 20μg protein lysates were electrophoresed on SDS-PAGE and transferred to Immobilon-P membranes (Millipore). The membranes were then probed with primary and secondary antibodies.

4.6 Immunofluorescent Microscopy:

Cells were seeded onto glass bottom plates (Cellvis), grown for 24 hours and exposed to 5mJ/cm^2 UV radiation. Then once it was the appropriate time after 5mJ/cm2 UV exposure, the cells were incubated in 4% formaldehyde for 15 minutes. Then the cells were permeabilized with 0.1% Triton X for 10 minutes. Next, the cells were blocked with 3% BSA and incubated with primary antibody overnight at 4°C. The next day, the cells were incubated with fluorescent secondary antibodies (1:500) for 1 hour

and stained with 300 nM DAPI (Thermo Fisher D1306) for 9 minutes. Cells were imaged using the Carl Zeiss 700 confocal microscope using the 40x (1.4 NA Oil) objective. Foci and intensity analyses were completed using ImageJ.

4.7 Subcellular Fractionation:

Cells were seeded and grown for 24 hours before being exposed to 5mJ/cm^2 and incubated for the appropriate time after radiation. Whole cell lysates were prepared by washing cells in cold 1XPBS before mechanically harvesting the cells in Subcellular Fractionation Buffer (HEPES, KCl, MgCl2, EDTA, EGA, pH 7.4, 1mM DTT, protease inhibitor, and phosphatase inhibitor). Nuclear and cytoplasmic lysates were separated through centrifugation. 20µg protein lysates were electrophoresed on SDS-PAGE and transferred to Immobilon-P membranes (Millipore). The membranes were then probed with primary and secondary antibodies.

4.8 mRNA Quantification

Cell were lysed using Trizol (Invitrogen) and RNA isolated with the RNeasy kit (Qiagen). Two micrograms of RNA were reverse transcribed using the iScript™ cDNA Synthesis Kit (Bio-Rad). Quantitative reverse transcription-PCR was performed in triplicate with the TaqMan™ FAM-MGB Gene Expression Assay (Applied Biosystems) and C1000 Touch Thermal Cycler (Bio-Rad). The following probes (Thermo Scientific) were used: ACTB (Hs01060665_g1), POLH (Hs00197814_m1), POLK (Hs00211965_m1), CHEK1 (Hs00967506_m1), XPA (Hs00166045_m1)

4.9 UV Radiation:

Cells were washed with 1XPBS and then irradiated using the UV Stratalinker 2400.

4.10 Statistical Analysis:

Statistical significance was determined using student's t-test. P values less than or equal to 0.05 were reported as significant.

Supplementary Materials: The following are available online, Figure S1: Higher expression of ATR/ATM mRNA correlates to an increase in UV damage repair pathways gene expression., Figure S2: hTERT HFK β-HPV 8E6-HA tag confirmation., Figure S3: β-HPV 8E6 attenuates p53 abundance., Figure S4: β-HPV 8E6 increases phosphorylation of RPA32., Figure S5: β-HPV 8E6 decreases XPA phosphorylation in U2OS cells., Figure S6: β-HPV 8E6 attenuates XPA localization in U2OS cells., Figure S7 β-HPV 8E6 does not broadly alter TLS proteins abundance.

Author Contributions: Conceptualization, N.A.W.; Resources, N.A.W.; Supervision, N.A.W.; Funding acquisition, N.A.W.; Investigation, J.A.S., V.M., D.D., C.H.; Validation, J.A.S., V.M., D.D., C.H.; Writing-original draft preparation, J.A.S., N.A.W.; Writing- review and editing, J.S., N.A.W., C.H., D.D., V.M.; Visualization, J.A.S.;

Funding: We would like to thank the Terry Johnson Basic Cancer Research Center and the Les Clow family for their support of this project. We also received support from a career development award provided by the United States' Department of Defense's Congressionally Directed Medical Research Program's Peer Reviewed Cancer Research Program (CMDRP PRCRP CA160224 (NW)).

Acknowledgments: Special thanks to Michael Underbrink for providing hTERT HFKs.

Conflicts of Interest: The authors declare no conflict of interest. Human foreskin keratinocytes were derived from anonymous donors under ethical guidelines approved by the Kansas State University's Insititional Review Bard (Protocol #7960).

References

1. de Villiers, E.-M. Cross-roads in the classification of papillomaviruses. *Virology* **2013**, *445*, 2–10.

2. Bernard, H.-U.; Burk, R.D.; Chen, Z.; van Doorslaer, K.; Hausen, H. zur; de Villiers, E.-M. Classification of papillomaviruses (PVs) based on 189 PV types and proposal of taxonomic amendments. *Virology* **2010**, *401*, 70–79.
3. de Villiers, E.-M.; Fauquet, C.; Broker, T.R.; Bernard, H.-U.; zur Hausen, H. Classification of papillomaviruses. *Virology* **2004**, *324*, 17–27.
4. Bzhalava, D.; Eklund, C.; Dillner, J. International standardization and classification of human papillomavirus types. *Virology* **2015**, *476*, 341–344.
5. Munger, K.; Baldwin, A.; Edwards, K.M.; Hayakawa, H.; Nguyen, C.L.; Owens, M.; Grace, M.; Huh, K. Mechanisms of Human Papillomavirus-Induced Oncogenesis. *J. Virol.* **2004**, *78*, 11451–11460.
6. Gheit, T. Mucosal and Cutaneous Human Papillomavirus Infections and Cancer Biology. *Front. Oncol.* **2019**, *9*, 355.
7. Brianti, P.; Flammineis, E.D.; Mercuri, S.R. Review of HPV-related diseases and cancers. 6.
8. Egawa, N.; Doorbar, J. The low-risk papillomaviruses. *Virus Res.* **2017**, *231*, 119–127.
9. Longworth, M.S.; Laimins, L.A. Pathogenesis of Human Papillomaviruses in Differentiating Epithelia. *Microbiol. Mol. Biol. Rev.* **2004**, *68*, 362–372.
10. Muñoz, N.; Castellsagué, X.; de González, A.B.; Gissmann, L. Chapter 1: HPV in the etiology of human cancer. *Vaccine* **2006**, *24*, S1–S10.
11. Duensing, S.; Münger, K. Mechanisms of genomic instability in human cancer: Insights from studies with human papillomavirus oncoproteins: Genomic Instability and Cervical Cancer. *Int. J. Cancer* **2004**, *109*, 157–162.
12. Wendel, S.O.; Wallace, N.A. Loss of Genome Fidelity: Beta HPVs and the DNA Damage Response. *Front. Microbiol.* **2017**, *8*, 2250.
13. Pfister, H. Chapter 8: Human Papillomavirus and Skin Cancer. *JNCI Monogr.* **2003**, *2003*, 52–56.
14. Hufbauer, M.; Akgül, B. Molecular Mechanisms of Human Papillomavirus Induced Skin Carcinogenesis. *Viruses* **2017**, *9*, 187.
15. Srinidhi Shanmugasundaram; Jianxin You Targeting Persistent Human Papillomavirus Infection. *Viruses* **2017**, *9*, 229.
16. Howley, P.M.; Pfister, H.J. Beta genus papillomaviruses and skin cancer. *Virology* **2015**, *479–480*, 290–296.
17. Weissenborn, S.J.; Nindl, I.; Purdie, K.; Harwood, C.; Proby, C.; Breuer, J.; Majewski, S.; Pfister, H.; Wieland, U. Human Papillomavirus-DNA Loads in Actinic Keratoses Exceed those in Non-Melanoma Skin Cancers. *J. Invest. Dermatol.* **2005**, *125*, 93–97.
18. Rollison, D.E.; Viarisio, D.; Amorrortu, R.P.; Gheit, T.; Tommasino, M. An Emerging Issue in Oncogenic Virology: the Role of Beta Human Papillomavirus Types in the Development of Cutaneous Squamous Cell Carcinoma. *J. Virol.* **2019**, *93*, e01003-18, /jvi/93/7/JVI.01003-18.atom.
19. Lomas, A.; Leonardi-Bee, J.; Bath-Hextall, F. A systematic review of worldwide incidence of nonmelanoma skin cancer: Worldwide incidence of nonmelanoma skin cancer. *Br. J. Dermatol.* **2012**, *166*, 1069–1080.
20. Apalla, Z.; Lallas, A.; Sotiriou, E.; Lazaridou, E.; Ioannides, D. Epidemiological trends in skin cancer. *Dermatol. Pract. Concept.* **2017**, *7*.
21. Patel, T.; Morrison, L.K.; Rady, P.; Tyring, S. Epidermodysplasia Verruciformis and Susceptibility to HPV. *Dis. Markers* **2010**, *29*, 199–206.
22. Nindl, I.; Rösl, F. Molecular Concepts of Virus Infections Causing Skin Cancer in Organ Transplant Recipients. *Am. J. Transplant.* **2008**, *8*, 2199–2204.

23. Bouwes Bavinck, J.N.; Feltkamp, M.; Struijk, L.; ter Schegget, J. Human Papillomavirus Infection and Skin Cancer Risk in Organ Transplant Recipients. *J. Investig. Dermatol. Symp. Proc.* **2001**, *6*, 207–211.
24. Tomaić, V. Functional Roles of E6 and E7 Oncoproteins in HPV-Induced Malignancies at Diverse Anatomical Sites. *Cancers* **2016**, *8*, 95.
25. Meyers, J.M.; Spangle, J.M.; Munger, K. The Human Papillomavirus Type 8 E6 Protein Interferes with NOTCH Activation during Keratinocyte Differentiation. *J. Virol.* **2013**, *87*, 4762–4767.
26. Meyers, J.M.; Uberoi, A.; Grace, M.; Lambert, P.F.; Munger, K. Cutaneous HPV8 and MmuPV1 E6 Proteins Target the NOTCH and TGF-β Tumor Suppressors to Inhibit Differentiation and Sustain Keratinocyte Proliferation. *PLOS Pathog.* **2017**, *13*, e1006171.
27. Taute, S.; Pfister, H.J.; Steger, G. Induction of Tyrosine Phosphorylation of UV-Activated EGFR by the Beta-Human Papillomavirus Type 8 E6 Leads to Papillomatosis. *Front. Microbiol.* **2017**, *8*, 2197.
28. Howie, H.L.; Koop, J.I.; Weese, J.; Robinson, K.; Wipf, G.; Kim, L.; Galloway, D.A. Beta-HPV 5 and 8 E6 Promote p300 Degradation by Blocking AKT/p300 Association. *PLoS Pathog.* **2011**, *7*, e1002211.
29. Wallace, N.A.; Robinson, K.; Howie, H.L.; Galloway, D.A. HPV 5 and 8 E6 Abrogate ATR Activity Resulting in Increased Persistence of UVB Induced DNA Damage. *PLoS Pathog.* **2012**, *8*, e1002807.
30. Wallace, N.A.; Gasior, S.L.; Faber, Z.J.; Howie, H.L.; Deininger, P.L.; Galloway, D.A. HPV 5 and 8 E6 expression reduces ATM protein levels and attenuates LINE-1 retrotransposition. *Virology* **2013**, *443*, 69–79.
31. Stauffer, D.; Chang, B.; Huang, J.; Dunn, A.; Thayer, M. p300/CREB-binding Protein Interacts with ATR and Is Required for the DNA Replication Checkpoint. *J. Biol. Chem.* **2007**, *282*, 9678–9687.
32. Marechal, A.; Zou, L. DNA Damage Sensing by the ATM and ATR Kinases. *Cold Spring Harb. Perspect. Biol.* **2013**, *5*, a012716–a012716.
33. Blackford, A.N.; Jackson, S.P. ATM, ATR, and DNA-PK: The Trinity at the Heart of the DNA Damage Response. *Mol. Cell* **2017**, *66*, 801–817.
34. O'Connor, M.J. Targeting the DNA Damage Response in Cancer. *Mol. Cell* **2015**, *60*, 547–560.
35. Hufbauer, M.; Cooke, J.; van der Horst, G.T.J.; Pfister, H.; Storey, A.; Akgül, B. Human papillomavirus mediated inhibition of DNA damage sensing and repair drives skin carcinogenesis. *Mol. Cancer* **2015**, *14*, 183.
36. Ramasamy, K.; Shanmugam, M.; Balupillai, A.; Govindhasamy, K.; Gunaseelan, S.; Muthusamy, G.; Robert, B.; Nagarajan, R. Ultraviolet radiation-induced carcinogenesis: Mechanisms and experimental models. *J. Radiat. Cancer Res.* **2017**, *8*, 4.
37. Sugitani, N.; Sivley, R.M.; Perry, K.E.; Capra, J.A.; Chazin, W.J. XPA: A key scaffold for human nucleotide excision repair. *DNA Repair* **2016**, *44*, 123–135.
38. Park, J.-M.; Kang, T.-H. Transcriptional and Posttranslational Regulation of Nucleotide Excision Repair: The Guardian of the Genome against Ultraviolet Radiation. *Int. J. Mol. Sci.* **2016**, *17*, 1840.
39. Göhler, T.; Sabbioneda, S.; Green, C.M.; Lehmann, A.R. ATR-mediated phosphorylation of DNA polymerase η is needed for efficient recovery from UV damage. *J. Cell Biol.* **2011**, *192*, 219–227.
40. Tonzi, P.; Huang, T.T. Role of Y-family translesion DNA polymerases in replication stress: Implications for new cancer therapeutic targets. *DNA Repair* **2019**, *78*, 20–26.
41. Akgül, B.; Kirschberg, M.; Storey, A.; Hufbauer, M. Human papillomavirus type 8 oncoproteins E6 and E7 cooperate in downregulation of the cellular checkpoint kinase-1: HPV8 downregulates Chk1. *Int. J. Cancer* **2019**, *145*, 797–806.

42. Barretina, J.; Caponigro, G.; Stransky, N.; Venkatesan, K.; Margolin, A.A.; Kim, S.; Wilson, C.J.; Lehár, J.; Kryukov, G.V.; Sonkin, D.; et al. The Cancer Cell Line Encyclopedia enables predictive modelling of anticancer drug sensitivity. *Nature* **2012**, *483*, 603–607.
43. Cerami, E.; Gao, J.; Dogrusoz, U.; Gross, B.E.; Sumer, S.O.; Aksoy, B.A.; Jacobsen, A.; Byrne, C.J.; Heuer, M.L.; Larsson, E.; et al. The cBio Cancer Genomics Portal: An Open Platform for Exploring Multidimensional Cancer Genomics Data: Figure 1. *Cancer Discov.* **2012**, *2*, 401–404.
44. Gao, J.; Aksoy, B.A.; Dogrusoz, U.; Dresdner, G.; Gross, B.; Sumer, S.O.; Sun, Y.; Jacobsen, A.; Sinha, R.; Larsson, E.; et al. Integrative Analysis of Complex Cancer Genomics and Clinical Profiles Using the cBioPortal. *Sci. Signal.* **2013**, *6*, pl1–pl1.
45. Abraham, R.T. Cell cycle checkpoint signaling through the ATM and ATR kinases. *Genes Dev.* **2001**, *15*, 2177–2196.
46. Cortez, D. Requirement of ATM-Dependent Phosphorylation of Brca1 in the DNA Damage Response to Double-Strand Breaks. *Science* **1999**, *286*, 1162–1166.
47. Canman, C.E. Activation of the ATM Kinase by Ionizing Radiation and Phosphorylation of p53. *Science* **1998**, *281*, 1677–1679.
48. Tibbetts, R.S.; Brumbaugh, K.M.; Williams, J.M.; Sarkaria, J.N.; Cliby, W.A.; Shieh, S.-Y.; Taya, Y.; Prives, C.; Abraham, R.T. A role for ATR in the DNA damage-induced phosphorylation of p53. *Genes Dev.* **1999**, *13*, 152–157.
49. Lavin, M.F.; Gueven, N. The complexity of p53 stabilization and activation. *Cell Death Differ.* **2006**, *13*, 941–950.
50. Awasthi, P.; Foiani, M.; Kumar, A. ATM and ATR signaling at a glance. *J. Cell Sci.* **2015**, 9.
51. Wallace, N.A.; Robinson, K.; Galloway, D.A. Beta Human Papillomavirus E6 Expression Inhibits Stabilization of p53 and Increases Tolerance of Genomic Instability. *J. Virol.* **2014**, *88*, 6112–6127.
52. Griewank, K.G.; Murali, R.; Schilling, B.; Schimming, T.; Möller, I.; Moll, I.; Schwamborn, M.; Sucker, A.; Zimmer, L.; Schadendorf, D.; et al. TERT Promoter Mutations Are Frequent in Cutaneous Basal Cell Carcinoma and Squamous Cell Carcinoma. *PLoS ONE* **2013**, *8*, e80354.
53. Gatei, M.; Scott, S.P.; Filippovitch, I.; Soronika, N.; Lavin, M.F.; Weber, B.; Khanna, K.K. Role for ATM in DNA Damage-induced Phosphorylation of BRCA1. *7*.
54. Matsuoka, S.; Rotman, G.; Ogawa, A.; Shiloh, Y.; Tamai, K.; Elledge, S.J. Ataxia telangiectasia-mutated phosphorylates Chk2 in vivo and in vitro. *Proc. Natl. Acad. Sci.* **2000**, *97*, 10389–10394.
55. Liu, S.; Shiotani, B.; Lahiri, M.; Maréchal, A.; Tse, A.; Leung, C.C.Y.; Glover, J.N.M.; Yang, X.H.; Zou, L. ATR Autophosphorylation as a Molecular Switch for Checkpoint Activation. *Mol. Cell* **2011**, *43*, 192–202.
56. Stokes, M.P.; Rush, J.; MacNeill, J.; Ren, J.M.; Sprott, K.; Nardone, J.; Yang, V.; Beausoleil, S.A.; Gygi, S.P.; Livingstone, M.; et al. Profiling of UV-induced ATM/ATR signaling pathways. *Proc. Natl. Acad. Sci.* **2007**, *104*, 19855–19860.
57. Zhao, H.; Piwnica-Worms, H. ATR-Mediated Checkpoint Pathways Regulate Phosphorylation and Activation of Human Chk1. *Mol. Cell. Biol.* **2001**, *21*, 4129–4139.
58. Iyer, D.; Rhind, N. The Intra-S Checkpoint Responses to DNA Damage. *Genes* **2017**, *8*, 74.
59. Xiao, Z.; Chen, Z.; Gunasekera, A.H.; Sowin, T.J.; Rosenberg, S.H.; Fesik, S.; Zhang, H. Chk1 Mediates S and G 2 Arrests through Cdc25A Degradation in Response to DNA-damaging Agents. *J. Biol. Chem.* **2003**, *278*, 21767–21773.
60. Shen, T.; Huang, S. The Role of Cdc25A in the Regulation of Cell Proliferation and Apoptosis. *Anticancer Agents Med. Chem.* **2012**, *12*, 631–639.

61. Lee, T.-H.; Park, J.-M.; Leem, S.-H.; Kang, T.-H. Coordinated regulation of XPA stability by ATR and HERC2 during nucleotide excision repair. *Oncogene* **2014**, *33*, 19–25.
62. Shell, S.M.; Li, Z.; Shkriabai, N.; Kvaratskhelia, M.; Brosey, C.; Serrano, M.A.; Chazin, W.J.; Musich, P.R.; Zou, Y. Checkpoint Kinase ATR Promotes Nucleotide Excision Repair of UV-induced DNA Damage via Physical Interaction with Xeroderma Pigmentosum Group A. *J. Biol. Chem.* **2009**, *284*, 24213–24222.
63. Bertoletti, F.; Cea, V.; Liang, C.-C.; Lanati, T.; Maffia, A.; Avarello, M.D.M.; Cipolla, L.; Lehmann, A.R.; Cohn, M.A.; Sabbioneda, S. Phosphorylation regulates human polη stability and damage bypass throughout the cell cycle. *Nucleic Acids Res.* **2017**, *45*, 9441–9454.
64. Tonzi, P.; Yin, Y.; Lee, C.W.T.; Rothenberg, E.; Huang, T.T. Translesion polymerase kappa-dependent DNA synthesis underlies replication fork recovery. *eLife* **2018**, *7*, e41426.
65. Hasche, D.; Vinzón, S.E.; Rösl, F. Cutaneous Papillomaviruses and Non-melanoma Skin Cancer: Causal Agents or Innocent Bystanders? *Front. Microbiol.* **2018**, *9*, 874.
66. Nindl, I.; Gottschling, M.; Stockfleth, E. Human Papillomaviruses and Non-Melanoma Skin Cancer: Basic Virology and Clinical Manifestations. *Dis. Markers* **2007**, *23*, 247–259.
67. Rodríguez-Rodríguez, D.; Ramírez-Solís, R.; Garza-Elizondo, M.; Garza- Rodríguez, M.; Barrera- Saldaña, H. Genome editing: A perspective on the application of CRISPR/Cas9 to study human diseases (Review). *Int. J. Mol. Med.* **2019**.
68. Friedberg, E.C. Suffering in silence: the tolerance of DNA damage. *Nat. Rev. Mol. Cell Biol.* **2005**, *6*, 943–953.
69. Stallons, L.J.; McGregor, W.G. Translesion Synthesis Polymerases in the Prevention and Promotion of Carcinogenesis. *J. Nucleic Acids* **2010**, *2010*, 1–10.
70. Zhang, Y.; Yuan, F.; Wu, X.; Wang, M.; Rechkoblit, O.; Taylor, J.-S.; Geacintov, N.E.; Wang, Z. Error-free and error-prone lesion bypass by human DNA polymerase κ in vitro. 9.
71. Lee, K.M.; Choi, K.H.; Ouellette, M.M. Use of exogenous hTERT to immortalize primary human cells. *Cytotechnology* **2004**, *45*, 33–38.
72. Pestana, A.; Vinagre, J.; Sobrinho-Simões, M.; Soares, P. TERT biology and function in cancer: beyond immortalisation. *J. Mol. Endocrinol.* **2017**, *58*, R129–R146.
73. Pópulo, H.; Boaventura, P.; Vinagre, J.; Batista, R.; Mendes, A.; Caldas, R.; Pardal, J.; Azevedo, F.; Honavar, M.; Guimarães, I.; et al. TERT Promoter Mutations in Skin Cancer: The Effects of Sun Exposure and X-Irradiation. *J. Invest. Dermatol.* **2014**, *134*, 2251–2257.
74. Wang, J.; Dupuis, C.; Tyring, S.K.; Underbrink, M.P. Sterile α Motif Domain Containing 9 Is a Novel Cellular Interacting Partner to Low-Risk Type Human Papillomavirus E6 Proteins. *PLOS ONE* **2016**, *11*, e0149859.
75. Scott, G.A.; Laughlin, T.S.; Rothberg, P.G. Mutations of the TERT promoter are common in basal cell carcinoma and squamous cell carcinoma. *Mod. Pathol.* **2014**, *27*, 516–523.
76. Forment, J.V.; Walker, R.V.; Jackson, S.P. A high-throughput, flow cytometry-based method to quantify DNA-end resection in mammalian cells. *Cytometry A* **2012**, *81A*, 922–928.